2-5 September 2013, Aalborg, Denmark

Proceedings of the 10th European Wave and Tidal Energy Conference

Conference host:

DEPARTMENT OF CIVIL ENGINEERING
AALBORG UNIVERSITY

Website host on behalf
of the Executive Committee:

UNIVERSITY OF
Southampton

www.ewtec.org/ewtec2013

Published by Technical Committee of the European Wave and Tidal Energy Conference

Copyright © 2013 European Wave and Tidal Energy Conference

ISSN 2309-1983

Development of Polychromatic Irregular Waves for Testing OWC Bidirectional Turbines at a Land-Based Test Facility

Judith R. Farman[†*], João A. Teixeira[†], James F. Whidborne[†], David Mba[†] and Shahab Natanzi[*]
[†]Cranfield University, School of Engineering, Bedfordshire, MK43 OAL, U.K.
E-mail: j.a.amaral.teixeira@cranfield.ac.uk
[*]Dresser-Rand Company Ltd, Peterborough, PE4 5HG, U.K.
E-mail: jfarman@dresser-rand.com, snatanzi@dresser-rand.com

***Abstract*—This paper presents the development of a control strategy that allows a dedicated oscillating water column turbine test facility to produce polychromatic waves. This facility allows testing of bi-directional turbines under transient conditions, validation of computational fluid dynamics simulations and testing of turbine control strategies under realistic sea states. The test facility employs a pneumatic wave generator (of unique design) to simulate the air flow of an oscillating water column. This work describes the methodology to create wave time series of various spectra that replicate a range of wave states at various geographical locations employing this rig.**

***Index Terms*—OWC, test-facility, turbine, polychromatic waves**

NOMENCLATURE

η	wave elevation (m)
λ	wave length (m)
ϕ	phase shift (rad)
ρ	density of water (kg/m^3)
a	wave amplitude(m)
A_{PM}	Pierson-Moskowitz spectrum coefficient A
B_{PM}	Pierson-Moskowitz spectrum coefficient B
f	frequency (Hz)
g	gravity (m/s^2)
H_{avg}	wave height average (m)
S_B	Brentschneider spectrum (m^2/s or m^2/Hz)
S_{PM}	Pierson-Moskowitz spectrum (m^2/s or m^2/Hz)
T	wave period (s)
t	time (s)
T_{avg}	period average (s)
$U_{19.5}$	wind speed at 19.5m above the sea level (m/s^2)
w	wave vertical velocity (m/s)
x	position (m)

I. INTRODUCTION

An oscillating water column (OWC) is made up of a partially submersed structure with an opening below the surface of the water such as to define an air chamber above the free surface of the sea. The chamber is connected to a bidirectional air turbine. This requires the employment of specialist turbines such as the Wells, Dennis Auld or HydroAir^{TM}designs. OWCs operate as a combined chain of energy conversion processes: wave to pneumatic, pneumatic to mechanical, and mechanical to electrical. Of these conversions the most critical for the overall efficiency of the device is the one which involves the air turbine.

There exist only a few facilities that have been reported which are designed to test the various OWC air turbines. Of these test facilities, some examine the performance of the turbines under steady flow conditions and the others under monochromatic bidirectional flow conditions. A full description of the existing test facilities will be given in Section II. Dresser-Rand Company Ltd, in conjunction with Cranfield University, has developed a test facility for the study of the variable radius turbine (VRT) commercialised under the HydroAir trademark. This test facility, referred to as the Pneumatic Wave Generator, was originally capable of producing monochromatic bidirectional flows; this work was presented by [1]; [2]; and [3]. The work presented here describes the control strategy development to enable this test facility to simulate a range of polychromatic air waves for a variety of wave spectra. It is believed that this is the first land-based test facility to enable testing of turbines under simulated realistic sea conditions.

This paper includes a literature review of the existing test facilities (Section II), followed by a review of the applicable theory describing wave spectra, the methodology for a derivation of a time series (Section III). In Section IV the hardware and control for the pneumatic wave generator (PWG) that enable polychromatic wave generation are presented. Finally, in Section V, simulation results are discussed for the averaging of waves within a rectangular section device in comparison with the point absorber assumption. This is followed by the verification of the accuracy of the test facility in reproducing a set of prescribed polychromatic waves.

II. OWC TURBINE TEST FACILITIES

Various test facilities have been developed to allow the characterisation of OWC turbines and to validate a range of numerical models describing their performance. This review identified six land-based facilities that have been reported as

©2013 European Wave and Tidal Energy Conference. Please refer to any applicable publisher terms of use.

being used for OWC testing employing a range of methods to produce reciprocating flows.

The facility described by [4] uses a 4kW variable speed centrifugal blower that can produce a flow rate of 1.1m^3/s and a pressure drop across the turbine of 2000Pa. Though this test facility could replicate a range of flow rates it did not produce bidirectional flows.

The test rig used by [5] consisted of an air bellow driven by a ram and hydraulic jack (Figure 1). Two 0.2m diameter Wells turbines with different solidities were tested with monochromatic flow oscillation with a frequency range of 0.2 to 1Hz.

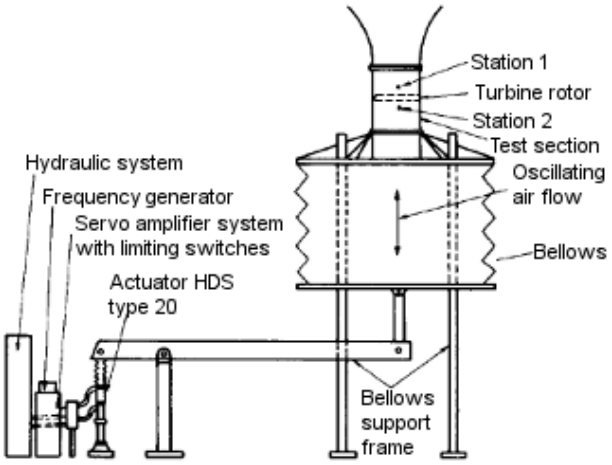

Fig. 1. Test rig using bellows [5].

Reference [6] completed unidirectional testing under steady flow conditions and then used numerical simulations to predict the turbine performance under irregular wave conditions, using a test rig consisting of a large piston of diameter 1.4m and stroke of 1.7m. References [7], [8], using the same test facility (Figure 2) reported a set of experiments using an impulse turbine with a tip radius of 298mm. The tests employed monochromatic waves with a 0.1Hz frequency. The experiments produced pressure drops of up to 1.8kPa with a maximum flow rate of 0.32m^3/s at a rotational speed of 370rad/s. It was deduced that since sea waves are irregular, it is important to characterise the turbine performance under transient conditions.

Reference [9] used a piston, with a diameter 1.25m, driven by a crank and rod connected to a disk with a number of holes at different eccentric distances to generate various flow rates. This created simulated sinusoidal waves of 0.404 to 2.46m^3/s. The test rig attained pressures that ranged from 0.77 to 4.3kPa. Although this test rig was used to test a twin unidirectional turbine, it is presumed that it could have been used to test bidirectional turbines.

The test facility used by [10] consists of a plenum chamber with honeycomb section. The air flow rate is generated by a centrifugal fan and then diverted using a bidirectional valve. The tests were conducted on a Wells turbine with turbine speeds ranging from 350 to 1,700rpm with a single period sine

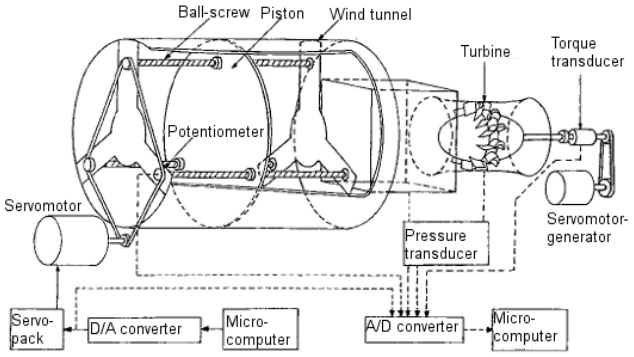

Fig. 2. Test rig using a piston [7].

wave of period 9.2s and velocity 8.4m/s. The turbine tested had a 597mm diameter.

Reference [11] presents work conducted at a test facility which consists of a large piston-cylinder, a settling chamber and a section to accommodate devices under test with a bell-mouthed end. The sinusoidal motion is created by an A.C. servo-motor driving the piston through mechanical translation, producing more than 1kPa and 0.7m^3/s. The authors reported problems with the test rig which meant the desired and actual frequencies were not perfectly matched. The rig was used to experiment with both turbines and orifice plates.

The Dresser-Rand and Cranfield University PWG test facility, presented initially by [1] and [2], produced a range of monochromatic pressure waves. To compare this test facility with the others, it is common (as seen above) to quote the capability of the test facility in terms of the flow rate and pressure waves generated. However, both of these values are functions of the turbine geometry, the instantaneous speed of the turbine rotor and the volume of the air chamber and ducting. The current turbine under test is a VRT and has a rotor diameter of 0.6m and can be tested with turbine speeds ranging between 100 to 1,500rpm. Static pressures have been measured up to $\pm$ 5kPa. This test facility is grid connected and exports generated power to the grid in compliance with G83/1 engineering recommendations.

Therefore, one may conclude that while a number of dedicated OWC turbine test facilities exist, only some of them can produce monochromatic pressure waves. At the time of writing, no turbine testing by employing polychromatic wave conditions at a land-based test facility is reported to have taken place. The test facilities surveyed are stated as producing peak flows of up to 2.46m^3/s and pressure drops of up to 4.3kPa. These figures are comparable with the PWG in its existing monochromatic control configuration. The work reported herein develops the test facility to produce polychromatic waves from a variety of wave spectra with a coefficient of determination of better than 0.99 (i.e., better than the measurement system capability). This enables land based testing of control strategies under sea conditions from different potential sites using different spectral types. In ad-

dition, seasonal variations can be incorporated by changing the parameters for the selected spectra. The next section will detail this further.

Note that an OWC's transfer function will modify the energy spectra as seen by the turbine however it is taken herein that the dynamics of the OWC under test are those of the PWG. The differences could be compensated for by modifying the incident wave dynamics. This would also require consideration of coupling effects. In this paper these differences are not considered any further.

III. Wave Theory

A. Wave Spectra

Realistic ocean wave profiles are not monochromatic (of single frequency); they are made up of a spectrum of frequencies and wave heights, each with a shift in the phase between 0 and 2π. A location at sea can be described as having a certain spectrum of waves but the terminology in this area is often confusing with the term spectrum referring to the energy spectrum, the variance density spectrum, and the amplitude spectrum. In this paper, the term spectrum shall refer to the variance density spectrum which has the units of m^2/s or m^2/Hz depending upon whether the spectrum is given in terms of wave frequency or wave period. These spectra are related in the following manner:[1]

$$S(f) = \frac{1}{f^2} S(T) \tag{1}$$

Reference [14] gives a basic introduction to wave climates which vary from location to location as the wave heights are dependent upon wind speed, wind duration and fetch.

The United Kingdom (UK) provides a good example of the variability of wave climate from one point on a coastline to another. The wave climate on the west coast of Cornwall is significantly different compared to that of the Northumberland coast. The waves on the Cornish coast can travel from their mid-Atlantic source, where the fetch distances can be considerable and would most likely be modelled using the Brentschneider or Pierson-Moskowitz spectra. However, on the east coast of the UK there is limited fetch distance over which the waves can be generated, and conditions are better modelled using the joint North Sea wave project (JONSWAP) spectra.

The general spectrum equations for the Pierson-Moskowitz and Brentschneider spectra presented by [12] and [13] are given directly below.

The Pierson-Moskowitz spectrum is defined as:

$$S(f)_{PM} = A_{PM} f^{-5} \exp^{-B_{PM} f^{-4}} \tag{2}$$

and uses the parameters A and B which are equal to:

$$A_{PM} = \frac{8.1\text{x}10^{-3} g^2}{(2\pi)^4} \tag{3}$$

$$B_{PM} = \frac{0.74}{(2\pi)^4} \left(\frac{g}{U_{19.5}} \right)^4 \tag{4}$$

[1]For further information on waves and associated spectra see [12] and [13]

where g is gravity and $U_{19.5}$ is the wind speed measured at 19.5m above sea water level. The Pierson-Moskowitz spectra models the behaviour of real sea waves in the Northern Atlantic Ocean [15] and describes a fully developed sea in deep water [12], [13], whereas the Brentschneider spectrum describes a developing sea [13].

The Brentschneider spectra,

$$S(f)_B = 3.437 \frac{H_{avg}^2}{T_{avg}^4} f^{-5} e^{-0.675 \left(\frac{1}{f T_{avg}} \right)^4} \tag{5}$$

was originally validated against the Pacific ocean in both the northern and southern hemispheres [16]. Predictions based on Brentschneider for North-Atlantic locations have resulted in overestimated sea states; however, improved accuracy was obtained for North Sea locations, and hence it was concluded that modelling North Sea sea-states by wind-waves spectra is relevant [17].

B. Wave series

References [18], [19] and [20] state that traditional linear wave theory (LWT) can be applied to oceanic gravity waves under the assumption of deep water. As such, a potential wave series can be generated from the spectrum either by applying an inverse fast Fourier transform (IFFT) or by summing a series of sine waves. The latter method is employed here. If one considers the inverse problem of generating a spectrum from a time series (when only one time series exists), then the spectral variance density must be estimated from one amplitude [12] and as such is equal to:

$$S(f) \approx \frac{1}{\Delta f} E\{\frac{1}{2} a_i^2\} \rightarrow \frac{1}{\Delta f} (\frac{1}{2} a_i^2) \tag{6}$$

Conversely, the amplitude can be estimated from the spectra:

$$a_i = \sqrt{2 S(f) \Delta f} \tag{7}$$

The wave elevation, η, at position, x, is then a time series generated from a sum of frequency components, f_i, with an amplitude, a_i, a wavelength λ_i and a random phase ϕ_i between 2π and zero:

$$\eta = \sum_{i=1}^{N} a_i \sin(2\pi f_i t - \frac{2\pi}{\lambda_i} x + \phi_i) \tag{8}$$

The vertical velocity of the wave is:

$$w = \sum_{i=1}^{N} 2\pi f_i a_i \cos(2\pi f_i t - \frac{2\pi}{\lambda_i} x + \phi_i) \tag{9}$$

C. Directionality of Waves

The assumption is made in this paper that the waves are perpendicular to the front edge of the device. The validity of this assumption is site dependent. Figure 3 shows the direction of waves at the Wave Hub wave energy test site measured between Aug 2009 and Jan 2010. One can therefore concluded that for certain sites this assumption may be valid.

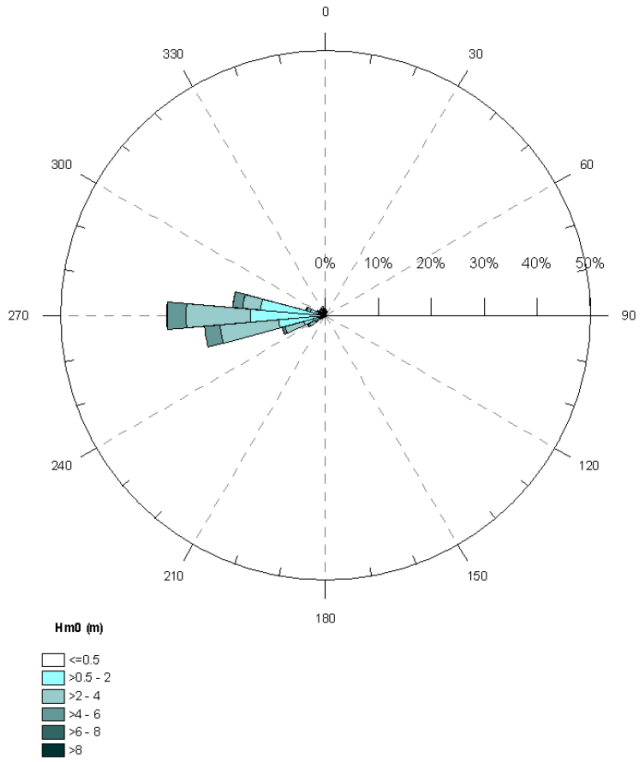

Fig. 3. Wave rose plot for the Wave Hub site between Aug 2009 and Jan 2010 [21]

IV. Pneumatic Wave Generator

A. PWG Hardware

The PWG is composed of a cylindrical air chamber made of glass reinforced plastic (GRP) with a rotary paddle that is controlled to produce oscillating air profiles (see Figure 6). The paddle periphery uses a brush seal to reduce leakage. The resulting air profile is then ducted though a square-to-round duct to the device under test. It is used to test the HydroAir™ VRT which uses a variable radius duct profile [22] (see Figures 4 and 5).

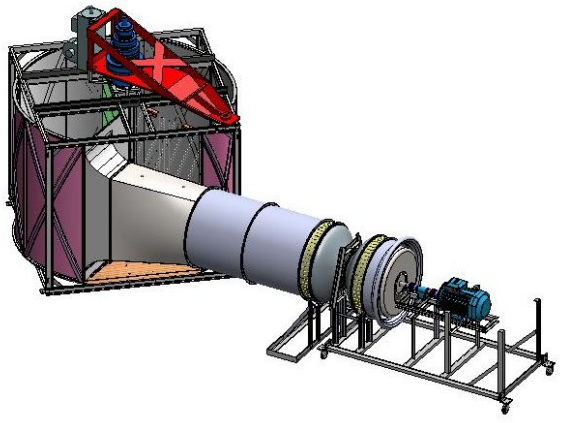

Fig. 4. CAD drawing of PWG test facility.

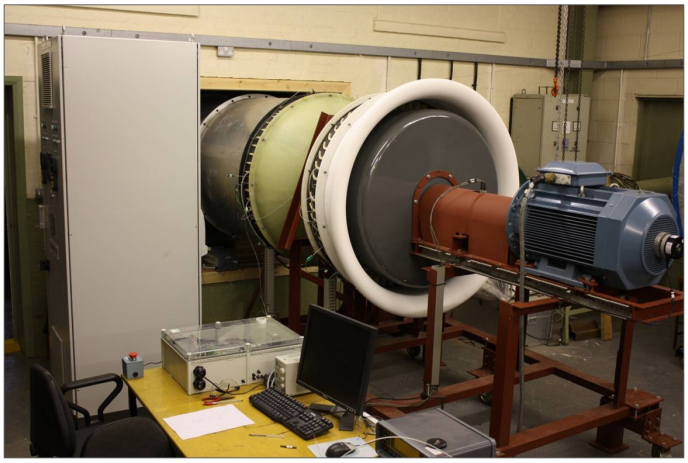

Fig. 5. PWG test facility turbine and power take-off.

The paddle is actuated by an induction generator with an integral position encoder connected via an input card to a back-to-back inverter. A single line diagram of the electrical equipment is shown in Figure 7. The inverter is controlled via a programmable logic controller (PLC) on a process field bus (PROFIBUS) connection.

Fig. 6. PWG test facility air chamber.

B. PWG Control

The PLC calculates the vertical position and velocity using the equations given in Section III for the wave profile from the required spectrum defined by the operator. The PLC program subsequently determines the speed reference value for the motor which is communicated on a PROFIBUS connection to the inverter drive at an update rate of 50ms and fed into a proportional integral derivative (PID) controller for the speed control loop of the motor. This approach was selected to

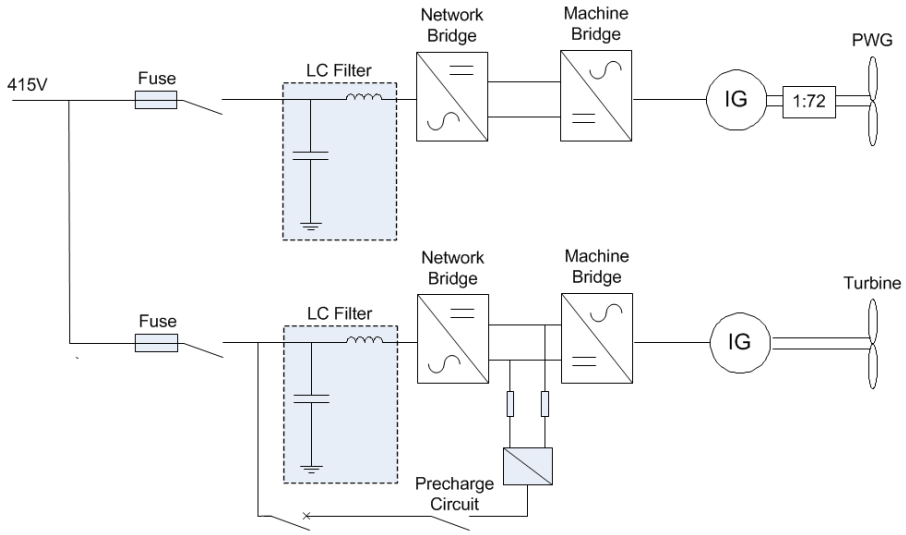

Fig. 7. Single line diagram.

avoid motor acceleration and deceleration phases inherent in the position control mode of the inverter. Protection software has been built into the control to ensure that the paddle does not overshoot the hard limits of the system. The system has been designed to be fail-safe; hence, loss of communication between the PLC and the inverter will result in the motor being controlled to a stationary position. The software has the ability to generate both monochromatic and polychromatic waves. The mean sea water level (SWL) is chosen to be the mid-point of the range of paddle sweeping angles. A limit switch positioned at the maximum swept angle is used to locate the paddle and then position control is used to locate the mid-point.

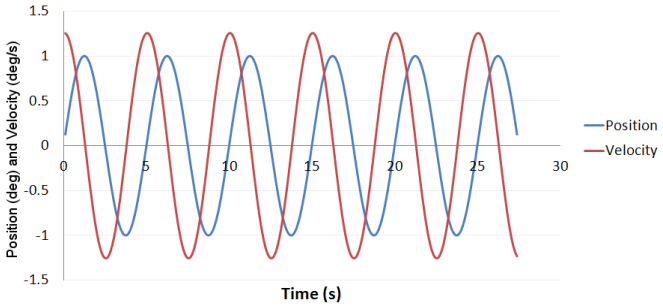

Fig. 8. Phase relationship between position and velocity.

In an ideal system, the position and velocity of a wave series are both zero at time equals zero. However, for a sine wave these values are always 90 degrees out of phase (see Figure 8). In the case where the position is taken to be zero, the speed needs to ramp up to maximum speed as fast as possible; however, this can activate hardware protection limits. The time taken to bring the speed up to the required value can create an offset in the wave position. The PWG system has a finite sweeping angle; therefore, to maximise the range of waves that can be produced, this offset should be minimised. In addition, this ensures that the mean SWL is constant across all waves.

One method to remove the offset is to use a ramp that has the same length as a multiple of the period of the wave in question. For example, a seven-second wave would require a ramp of 7, 14, 21 seconds etc. (see Figure 9). If a ramp of a different length is used, then an offset is introduced (see Figure 10). This can be carried over to the polychromatic wave scenario by multiplying each frequency component by its own ramp rate. The resulting output is shown in Figure 11, where a generic polychromatic wave is represented though its velocity and amplitude characteristics and where the desired polychromatic series signal is closely represented within 15 seconds.

C. Instrumentation

The turbine under test is connected to the National Grid (NG) using a back-to-back integrated gate bipolar transistor (IGBT) inverter decoupling the turbine speed from the frequency of the grid (see Figure 7). The inverter (and hence the generator and the turbine) are controlled using a PLC. The turbine is fitted with 64 pressure tappings connected to two 32 channel pressure scanners that incorporate digital thermal compensation within a range of $\pm$7kPa. The pressure scanners have a capability of 625 measurements per channel per second with a full scale accuracy of 0.06% [23]. The pressure ports are used to measure both static and total pressures at the guide vanes and static pressure upstream and downstream of the rotor. A number of the turbine guide vanes are fitted with four pressure tappings (see Figure 12). The spanwise locations of these tappings were determined from numerical studies of the flow through the guide vanes. The leading edge pressure probes are employed in estimating the volume flow. The main advantages of their position is their minimal

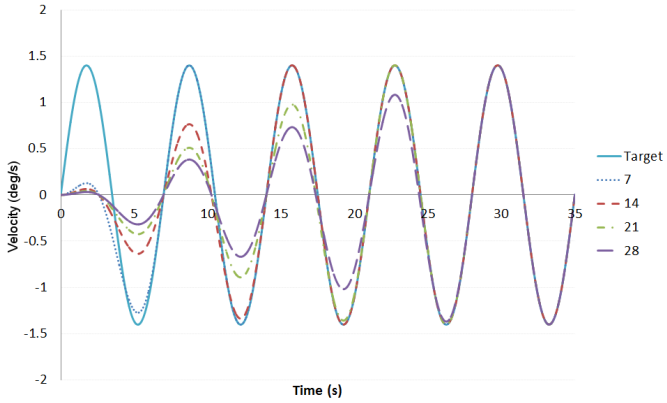

Fig. 9. A 7s wave with a ramp of 7s, 14s, 21s and 28s.

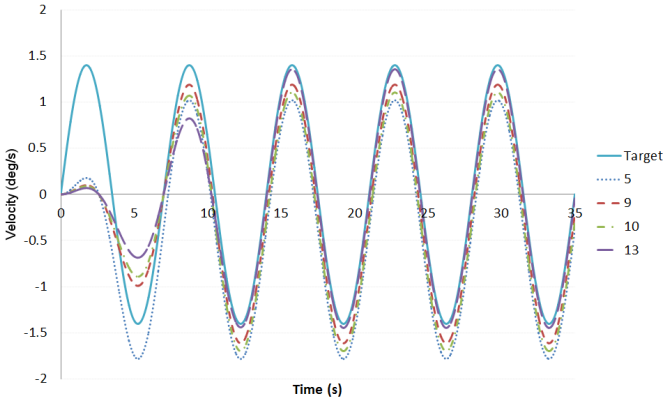

Fig. 10. A 7s wave with a ramp of 5s, 9s, 10s and 13s.

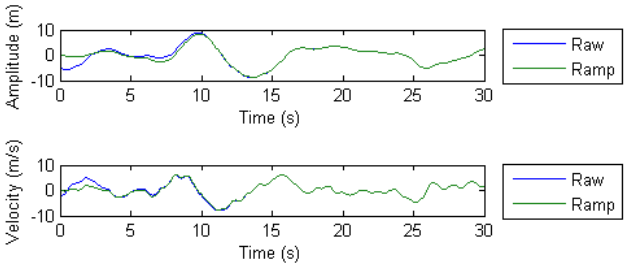

Fig. 11. Poly wave position and velocity.

effect on the flow, that the usual area of stagnation pressure behind the probe is reduced (potentially even eradicated) and there is an increase in their structural integrity. This latter point is extremely important for using total pressure ports on turbines to be commissioned in the ocean, where redundancy is important. Additional pressure measurements are taken at a number of locations from within the PWG chamber. A torque speed transducer and generator encoder are used to enable turbine measurements in isolation from the generator. The inverter cubicle has current transformers (CTs) and voltage transformers (VTs) on the machine and grid side connections in order to calculate the electrical power output. In addition, a power logger and power quality analyser can be used to monitor the output voltages and the degree of flicker and harmonics in the system. Barometric pressure is measured, as well as atmospheric temperature. A variety of measurements from the back-to-back inverter can be communicated to the data acquisition hardware. An additional encoder is used to measure the position of the PWG flap. The instrumentation data is acquired and processed via a bespoke human machine interface (HMI). IGBT inverters can cause problems with electromagnetic radiation (EMR); hence all instrumentation at the test facility was screened and low voltage signals were avoided wherever possible.

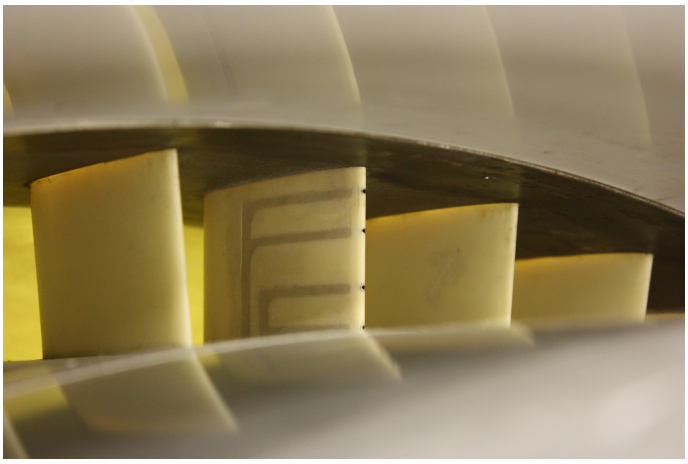

Fig. 12. Total pressure probes embedded in turbine blades.

V. Results

A. Generated Monochromatic Pressure Waves

Linear regression calculations were computed for a range of monochromatic waves for flow rates of 1.2 and 1.77m^3/s and a range of wave periods from 5 up to 12s. The coefficient of determination[2], R^2, between the desired position and actual paddle position is higher than 0.99 for all the monochromatic wave cases, and has a largest error of 2.5%. It can therefore be seen that the velocity set-point approach had no significant detrimental impact on the position accuracy.

The measurement of the instantaneous bulk flow is carried out through the use of a set of rake-like instrumented guide vanes. Figure 13 shows a time history of the dynamic pressure as calculated from the total and static pressure measurements on the chamber side (P1) and the atmosphere side (P2) of the turbine (see Equation 10). Each total pressure probe is upstream for only half of the wave cycle.

$$P_{dyn} = P_{tot} - P_{stat} \tag{10}$$

Notice how the downstream pressure signals follow closely to the corresponding upstream fluctuation. However, the vanes

[2]"R^2 is used to describe how well a regression line fits a set of data. An R^2 near 1.0 indicates that a regression line fits the data well, while an R^2 closer to 0 indicates a regression line does not fit the data very well."

trailing edge pressure shows a fluctuation due to the localised separation near the probe location. The standard deviation of the total pressure measurements at P1 as a function of the root mean square (RMS) pressure is shown in Figure 14. This quantity is lower than 1% for the pressure probes upstream of the turbine. As the flow changes direction it deteriorates to only 4% at its worst. This indicates that the velocity is relatively uniform across the annulus.

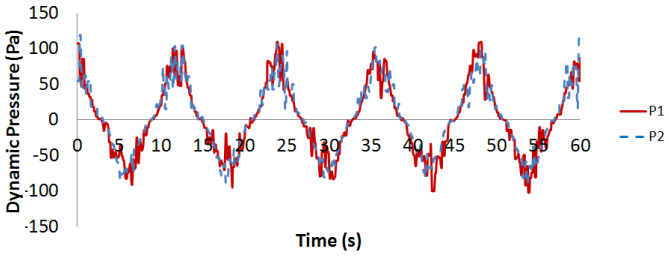

Fig. 13. Dynamic pressure measurements for a wave of 12s period and $1.8 m^3/s$ flow rate.

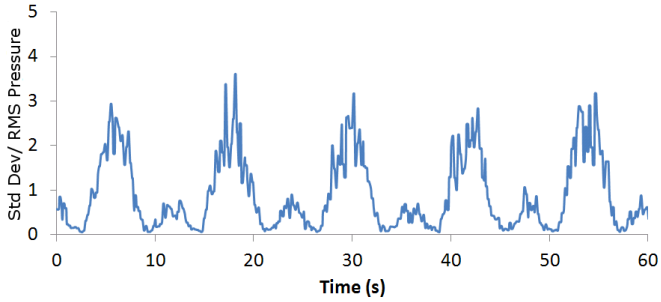

Fig. 14. Standard deviation of the total pressure measurements divided by the RMS pressure for a wave of 12s period and 1.8 m^3/s flow rate.

B. Generated Polychromatic Pressure Waves

Having demonstrated the validity of the speed control method, the test program expanded to demonstrate the feasibility of polychromatic pressure wave generation. The pressure plot for an irregular wave, generated from a Pierson-Moskowitz spectum with a wind speed of 15.4m/s measured at 19.5m above sea water level, is shown in Figure 15. The test was performed three times (V1,V2 and V3) and shows good repeatability. The amplitudes and phase shifts of each individual frequency are calculated via a Matlab script and then programmed into the PLC. This enables the test facility to repeat a wave series for back-to-back comparison testing. The rig could use a random number generator and calculate the amplitude and phase shift itself; however, this requires more computation and it was decided that this approach offered very little benefit compared to the one described above. The same method was implemented for a Brentschneider spectum and the resulting pressure wave time series is shown in Figure 16. For the results from the Pierson-Moskowitz spectrum testing (Figure 17) one can see that there is a strong correlation between the actual and desired position data and the line of best fit (R^2 equals 0.96). The proximity of this line of best fit to $y = x$ demonstrates that the PWG can be relied upon to deliver the required paddle position and, therefore, flow conditions.

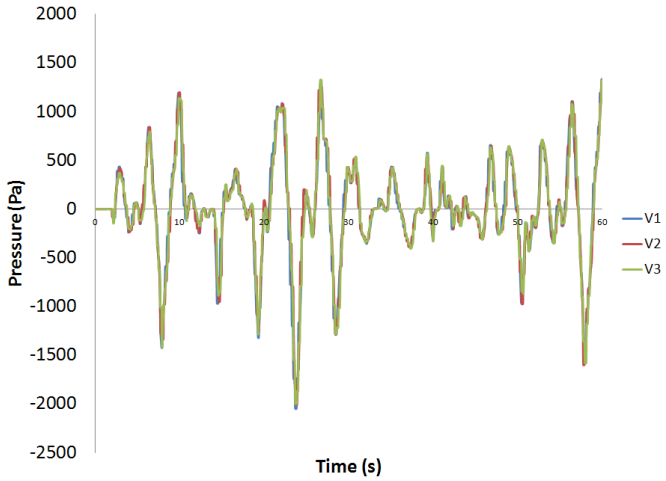

Fig. 15. Pressure plot for a scaled Pierson-Moskowitz derived irregular wave with a wind speed of 15.4 m/s.

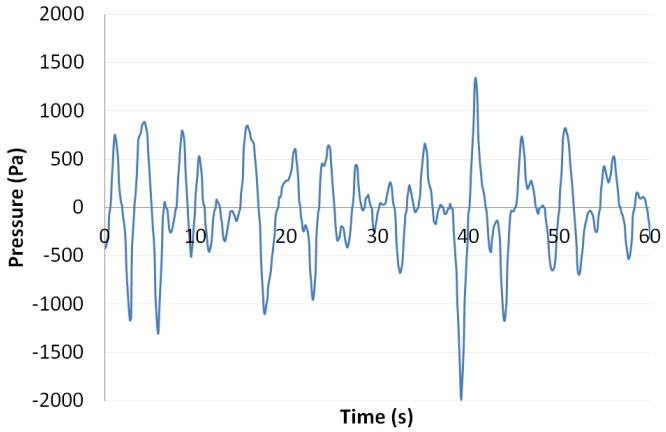

Fig. 16. Pressure plot for a scaled Brentschneider derived irregular wave with a significant wave height of 4.5m and and a peak period of 12 s.

VI. Conclusion

Implementing polychromatic waves with the PWG rig to test bidirectional turbines was proven with success. Pressure waves corresponding to a given sea level can be controlled to within 2% accuracy and to a high level of repeatability. The method uses speed control rather than position control for the reference. This test facility will enable the testing of control strategies as well as the investigation of the performance of self regulating OWC turbines in realistic operating conditions. For the control schemes, this type of testing prior to deployment in the ocean will increase the confidence in and reliability of

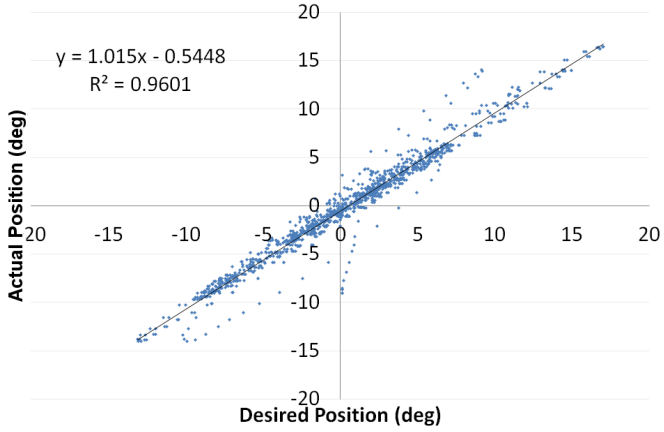

Fig. 17. Accuracy for a Pierson-Moskowitz wave.

the strategies employed in maximizing power while seeking to adhere to the quality of grid supply. In addition, the test facility will continue to be used to validate a range of theoretical models.

ACKNOWLEDGEMENTS

This research was conducted through the sponsorship of Dresser-Rand and the EPSRC (GR/T18424/01)

REFERENCES

[1] S. Herring, "Design and evaluation of turbines for use in OWC power plants," Ph.D. dissertation, Cranfield University, School of Engineering, Cranfield, Engineering, 2007.

[2] S. Herring and G. Laird, "A new test facility for evaluating turbines for use in OWC power plants," in *Proceedings of the 7th European Wave and Tidal Energy Conference, 11-13 September 2007.*, Porto, Portugal,, 2007.

[3] S. Natanzi, J. Teixeira, and G. Laird, "A novel high-efficiency impulse turbine for use in oscillating water column devices," in *Proceedings of the 9th European Wave and Tidal Energy Conference*. Southampton, UK: EWTEC, 5th - 9th September 2011.

[4] T. Dhanasekaran and M. Govardhan, "Computational analysis of performance and flow investigation on Wells turbine for wave energy conversion," *Renewable Energy*, vol. 30, 2005.

[5] S. Raghunathan and O. Ombaka, "Effect of frequency of air flow on the performance of the Wells turbine," *Int. J. Heat and Fluid Flow*, vol. 6, no. 2, pp. 127–132, 1985.

[6] H. Maeda, T. Setoguchi, M. Takao, K. Sakurada, T. Kim, and K. Kaneko, "Comparative study of turbines for wave energy conversion," *Journal of Thermal Science*, vol. 10, no. 1, 2001.

[7] H. Maeda, M. Takao, T. Setoguchi, K. Kaneko, and T. Kim, "Impulse turbine for wave power conversion with air flow rectification system," in *Proceedings of the Eleventh (2001) International Offshore and Polar Engineering Conference*, Stavanger, Norway, 2001.

[8] T. Setoguchi, M. Takao, Y. Kinoue, and K. Kaneko, "Study on an impulse turbine for wave energy conversion," *International Journal of Offshore and Polar Engineering*, vol. 10, no. 2, 2000.

[9] K. Mala, J. Jayaraj, V. Jayashankar, S. Muruganandam, T.M.and Santhakumar, M. Ravindran, M. Takao, T. Setoguchi, K. Toyota, and S. Nagata, "A twin unidirectional impulse turbine topology for OWC based wave energy plants - experimental validation and scaling," *Renewable Energy*, vol. 36, pp. 307 – 314, 2011.

[10] A. Thakker and R. Abdulhadi, "The performance of Wells turbine under bidirectional airflow," *Renewable Energy*, vol. 33, no. 11, pp. 2467–2474, 2008.

[11] Z. Liu, B.-S. Hyun, K.-Y. Hong, and Y.-Y. Lee, "Investigation on integrated system of chamber and turbine for OWC wave energy convertor," in *Proceedings of the Nineteenth (2009) International Offshore and Polar Engineering Conference*, June 21-26 2009.

[12] L. Holthuijsen, *Waves in Oceanic and Coastal Waters*. Cambridge: Cambridge University Press, 2007.

[13] M. McCormick, *Ocean Engineering Mechanics: with Applications*. Cambridge: Cambridge University Press, 2010.

[14] G. Pretor-Pinney, *The wavewatcher's companion*. London: Bloomsbury Publishing Plc, 2010.

[15] D. Valério, M. Mendes, P. Beirão, and J. Sá da Costa, "Identification and control of the AWS using neural network models," *Applied Ocean Research*, vol. 30, pp. 178–188, 2008.

[16] C. Brentschneider, "Revisions in wave forecasting: Deep and shallow water," in *Proc. 6th Int. Conf. Coastal Eng.*, 1958, pp. 30–67.

[17] J. Saulnier, P. Ricci, M. Pontes, and A. d. O. Falcão, "Spectral bandwidth and WEC performance assessment," in *Proceedings of the 7th European Wave and Tidal Energy Conference*, no. 1, 2007.

[18] F. Guerrini, "Numerical analysis of OWC devices for offshore applications," Master's thesis, University of Cranfield, 2009.

[19] H. Krogstad and O. Arntsen, *Linear Wave Theory*. Norwegian University of Science and Technology, 2000.

[20] E. Fantini, "Free surface flow CFD simulation for developing oscillating water column technology," Master's thesis, University of Cranfield, 2007.

[21] Halcrow Group Ltd, "Wave hub wave monitoring project, interim report number 3, Feb 2010," South West of England Regional Development Agency (SW RDA), Tech. Rep. Doc No 1 Rev 0, 2010. [Online]. Available: http://www.wavehub.co.uk/information-for-developers/

[22] C. Freeman, S. Herring, and K. Banks, "Impulse turbine design UK Pat. GB2440344A," British Patent GB2 440 344A, 2008. [Online]. Available: http://worldwide.espacenet.com

[23] *CANdaq III Pressure Scanner Acquisition System Installation and Operating Manual*, Chell Instruments Ltd, 2010. [Online]. Available: http://www.chell.co.uk

Cranfield University

CERES Research Repository **https://dspace.lib.cranfield.ac.uk/**

School of Aerospace, Transport and Manufacturing (SATM) Staff publications (SATM)

Development of polychormatic irregular waves for testing OWC bidirectional turbines at a land-based test facility

Farman, Judith R.

2013-09

Judith R. Farmany, Joao A. Teixeiray, James F. Whidborney, David Mbay and Shahab Natanzi. Development of polychormatic irregular waves for testing OWC bidirectional turbines at a land-based test facility. Prcoeedings of the 10th European Wave and Tidal Energy Conference, 2-5 September 2013, Aalborg, Denmark.

www.ewtec.org/wp-content/uploads/2014/02/EWTEC2013_Contents.pdf

Downloaded from CERES Research Repository, Cranfield University